Improving the Performance of Supported Ionic Liquid Phase (SILP) catalysts for the Ultra-Low-Temperature Water-Gas Shift Reaction Using Metal Salt Additives

Patrick Wolf[1], Manfred Aubermann[1], Moritz Wolf[1], Tanja Bauer[2], Dominik Blaumeiser[2], Robert Stepic[3,4], Christian R. Wick[3], David M. Smith[4], Ana-Sunčana Smith[3,4], Peter Wasserscheid[1], Jörg Libuda[2], and Marco Haumann[1*]

[1]Lehrstuhl für Chemische Reaktionstechnik, Friedrich-Alexander-Universität Erlangen-Nürnberg, Egerlandstraße 3, D-91058 Erlangen, Germany

[2]Lehrstuhl für Katalytische Grenzflächenforschung, Friedrich-Alexander-Universität Erlangen-Nürnberg, Egerlandstraße 3, D-91058 Erlangen, Germany

[3]PULS Gruppe, Department Physik und Interdisziplinäres Zentrum für Nanostrukturierte Filme IZNF, Friedrich-Alexander-Universität Erlangen-Nürnberg, Cauerstr. 3, D-91058 Erlangen, Germany

[4]Group for Computational Life Sciences, Division of Physical Chemistry, Ruđer Bošković Institute, Bijenička cesta 54, HR-10000 Zagreb, Croatia

Corresponding author: marco.haumann@fau.de

Keywords

Water-gas shift reaction, supported ionic liquid phase, ruthenium, copper halides, solubility

Abstract

Supported ionic liquid phase (SILP) catalyst systems containing homogeneous Ru-complexes dissolved in ionic liquids (ILs) catalyze the water-gas shift reaction (WGSR) at very low temperatures, i.e., between 120 to 160 °C. One limiting factor of the SILP WGS technology is the

low solubility of CO in most ionic liquids. To overcome this issue, we study the influence of different transition metal chloride additives on the activity of Ru-based WGS SILP catalysts. CuCl as additive was found to enhance the activity by almost 30 %. This increase in activity peaks at a CuCl addition of 4 M as a result of the interplay between increasing CO uptake in the ionic liquid film as evidenced by means of CO sorption and thermogravimetry, and the increasing, unfavorable ionic liquid acidity at too high CuCl concentrations. The respective chlorocuprate species were identified by means of *in situ* diffuse reflectance infrared Fourier transform spectroscopy (DRIFTS) in combination with density functional theory (DFT) calculations. We attribute the enhanced catalytic performance to cuprate ions that act as CO shuttles within the ionic liquid film.

Introduction

Hydrogen is an important resource for many processes like hydrocracking, ammonia and methanol production as well as metal fabrication and food production or electronics sector. [1-2] The constantly growing demand of hydrogen (around 65 Mt p.a. [3-4]) is still being supplied from fossil fuels via steam reforming, which is the primary route of hydrogen production nowadays. [2-3, 5] During steam reforming carbon monoxide is formed as coupling product, which can be a severe poison for many catalysts. For high purity hydrogen applications such as fuel cells or ammonia synthesis, CO has to be removed. Here, the water-gas shift reaction (WGSR) is the method of choice to lower the CO content via conversion of CO and H_2O to CO_2 and H_2. Due to the exothermic nature of the WGSR, low process temperatures around 150 °C and below would be desirable to obtain high equilibrium conversions. However, commercial heterogeneous catalysts must operate at temperatures between 200 °C and 450 °C. [6] In 2010, Werner et al. reported a new catalyst system which is based on the immobilization of a homogeneous Ru-complex in thin films of ionic liquid (IL). This catalyst allows operation at ultra-low temperatures of 120 °C and therefore

outperforms the state-of-the-art commercial catalysts. [7] These Supported Ionic Liquid Phase (SILP) catalysts consist of a thin IL film containing a homogeneous transition metal-complex which is dispersed on a highly porous substrate. [8] The extremely low vapor pressure of the IL prevents its stripping and leads to solid materials which are long-term stable, dry and free flowing. [8-10] However, one limiting factor can be the carbon monoxide solubility in the IL, which is known to be low for many permanent gases in most ILs. [11-12]

Already in 1960, Kohl and Riesenfeld described the so-called copper liquor process in great detail in which CO reacts reversibly with the cuprous ion complex $[Cu(NH_3)_2]^+$ under elevated pressures. [13] However, the main problem in this gas-liquid processes the stability of the Cu^+ ion, which is the active species for the reversible CO adsorption. [14] Another process for selective CO separation is the COSORB process described by Haase et al. [15] Here, CO is in equilibrium with the activating agent ($CuAlCl_4$) in a hydrocarbon solvent (typically toluene) under mild conditions. [16-17] Again, the main issue is the stability of the $CuAlCl_4$ complex, which is prone to react with impurities such as H_2O or H_2S. [14] A commercially well-established process for the selective CO recovery is the pressure swing adsorption (PSA) which is currently the dominating technical CO separation method. [18] In this process, the adsorbent consists of an activated alumina/carbon carrier which is impregnated with CuCl as the active chemisorption species. [19] Besides the above-mentioned processes, which are focusing on aluminous and cuprous compounds, various other possibilities for the selective and reversible binding of CO have been described in the literature. Benner et al. investigated the insertion of CO into the metal-metal bond of some palladium(I) or palladium(0) dimers [20], while Komatsu et al. reported the binding of CO to “double-sided” porphyrinatoiron(II) complexes. [21] Tyeklár et al. in turn described reversible reactions of CO with copper(I) complexes containing tris(2-pyirdylmethyl)-amine ligands. [22] In 2012, David et al. reported on the use of chlorocuprate imidazolium-based ILs for the absorption of CO. [23]

Interestingly, chlorocuprate compounds have already been synthesized and characterized since the 1960ies in various studies without addressing adsorption applications. [24-29] It was found that at low metal halide content, the formed species exhibit Lewis-basic behavior, while at high metal halide content they become Lewis-acidic. [29-30] It should be noted that CO binds reversibly via π-interactions to transition metal complexes. These bonds are typically of rather low strength and can be formed between e.g. d-block elements and ligands like CO. [19]

The aim of the present work is to push the performance of Ru-based SILP WGS catalysts by additives to the supported IL film that improve the CO uptake in the IL catalyst layer. In detail, we modify 1-butyl-2,3-dimethylimidazolium chloride ($[C_4C_1C_1Im]Cl$), which is the standard IL in SILP WGS systems based on previous studies [31], with a selection of transition metal chlorides resulting in the formation of the respective chlorometallate ILs. In particular, we focus on the influence of the different additives on the catalytic activity as a function of temperature. Observed effects on the catalytic performance are correlated with the CO uptake of the doped $[C_4C_1C_1Im]Cl$ as quantified by sorption and gravimetric studies. The different species formed under these conditions are assigned with the help of DRIFTS and DFT calculations.

Experimental

SILP catalyst preparation. All SILP catalysts were prepared in Schlenk flasks under argon atmosphere at ambient pressure and temperature. First, the $[C_4C_1C_1Im]Cl$ (purchased from Merck KgaA, LOT: 99/818) was dissolved in dichloromethane (DCM; Sigma-Aldrich, LOT: SZBG073AV) and stirred for 10 - 15 min. Subsequently, the precursor complex $[Ru(CO)_2Cl_3]_2$ (Alfa Aesar, LOT: X06C034) was dissolved in the mixture by adding further DCM and stirring for another 10 - 15 min. If an additive (Merck KgaA: $CoCl_2$, LOT: H02X026, 99.9 %; CuCl, LOT: A999739833, ≥ 97.0 %; $FeCl_2$, 0000021293, ≥ 98.0 %); $ZnCl_2$, LOT: B0124916814,

98.0 %; AnalaR Normapur: $NiCl_2$, LOT: 07E290005, ≥ 98.0 %) was added, the latter was dissolved using further 10 mL of DCM and the mixture was stirred for 60 – 90 min. Finally, the alumina support (ɤ-Al_2O_3, Sasol Germany GmbH, LOT: B39598) was added to the mixture and stirred shortly for 2 – 5 min to avoid mechanical stress of the support material. After removing the stirring bar, the solvent was removed in two steps using a rotary evaporator (step 1: 3 h, 40 °C, 900 mbar; step 2: 1 h, 40 °C, < 3 mbar). Subsequently, the free-flowing SILP catalyst was stored under argon atmosphere. The Ru-loading of the SILP catalyst was w_{Ru}= 0.02 $g_{Ru} g^{-1}_{support}$. The pore filling grade of the support, which describes the IL volume related to the total pore volume of the support material (V_{IL} $V_{support}^{-1}$), was α = 0.34. The molar amount of additive to IL (in mol L_{IL}^{-1}) was varied between 0.5 and 8 M corresponding to a molar ratio χ (in $mol_{additive}$ / mol_{IL}) of 0.04 – 1.4, respectively.

CO uptake measurements. As one possibility to measure the CO uptake of the catalysts, a pulse chemisorption setup was chosen. The measurement procedure is described in the DIN standard 66136-3. [32] In this work, the CO uptake was determined by following a pulse chemisorption analysis in an AutoChem 2920 device from Micrometrics®. 0.3 – 0.4 g of the prepared SILP catalyst have been placed in a u-bend quartz glass tube. A bed of glass wool prevented the discharge of the catalyst. It was ensured, that the catalyst bed was in the isothermal zone of the oven. For the chemisorption measurement, the sample was heated to 130 °C with a heating rate of 5 °C min^{-1} under a helium flow of 20 mL_N min^{-1}. When the measurement conditions were reached, the sample was dried for 80 minutes. After drying, the pulse experiment was started with a sample loop volume of 0.5 mL_N of CO. Between every pulse, the delay time was 6 minutes. The measured TCD signal of the eluting CO (as area and peak height) can be directly related to the amount of CO adsorbed by the sample under standard conditions ($cm^3_{N,\,CO}\ g^{-1}_{sample}$). The measurement is considered to be complete when two consecutive peaks have the same area and height. An exemplary graph of a

chemisorption experiment with a benchmark SILP system (no additives) is shown Figure S1 in the Supporting Information where the TCD signal is plotted over time. The maximum error was below 5 % and error bars have been omitted for the sake of clarity.

CO chemisorption was also conducted for various SILP catalysts and reference samples using a XEMIS sorption analyzer (Hiden Isochema).[33] The XEMIS analyzer allows for high-resolution thermogravimetric analysis (HRTGA) with a superior sensitivity of ± 0.1 µg and can be operated at low vacuum or pressures up to 200 bar at a maximum temperature of 500 °C. A total of ~200 mg of the particular samples was placed in a cylindrical stainless steel mesh sample holder, exposed to a flow of inert He at 27.3 $mL_N\ min^{-1}$ at 0.1 bar and subsequently heated to 130 °C (5 °C min^{-1}) for 6 h in order to remove adsorbed H_2O. The overall pressure was increased to 1 bar under a continuous flow of 100.0 $mL_N\ min^{-1}$ He and chemisorption of CO was monitored for 6 h after changing the flow to 100 $mL_N\ min^{-1}$ CO. The maximum weight increase during exposure to CO represents the maximum CO uptake of the particular samples and can be converted to a mass specific volumetric CO uptake by relating the measured weight increase to the mass of the dry sample after the preceding treatment under He atmosphere. Here, the maximum error was below 1 % and error bars have been omitted for the sake of clarity.

Catalytic evaluation. All catalytic experiments were carried out in a fixed-bed reactor setup (1.4571 stainless steel) with an inner diameter of 10 mm and a total volume of 26 mL. The reactor and its peripheral structures are depicted in Figure S5 in the Supporting Information. The gases CO (3.7, Linde AG) and N_2 (5.0, Linde AG) were dosed via mass flow controllers. Water was dosed with a liquid flow controller and mixed with N_2 utilizing a controlled evaporator mixer (CEM) unit from Bronkhorst. The gas mixture consisting of N_2, CO and water can either pass through a bypass-line (for reference measurement purposes) or the fixed-bed reactor. The catalyst samples were placed on a 0.5 µm frit to avoid particles from entering the downstream section. After the reactor

or the bypass-line respectively, the gas mixture was flowing through a condenser unit (T = 1.5 °C) in order to remove the moisture from the stream. Finally, the gas composition was analyzed by an Emerson X-Stream gas analyzer based on IR technology which allows for *in situ* measurement of the gas mixture. After the ramp-up phase under a low N_2 flow (50 mL_N min^{-1}), the reaction mixture was directed through the bypass-line in order to gain a reference point for the calculation of the catalytic activity. Subsequently, the gas stream was sent through the fixed-bed reactor and an automated temperature variation program was started (temperature variation from 120 °C as reference set point to 140 °C in 5 °C steps with a reference set point in-between each temperature). Every temperature stage was kept for 5 h, so that a total time-on-stream (TOS) of 45 h was reached. The results of such a typical characterization experiment can be seen for example in Figure 1.

The calculation of the SILP catalyst activity is based on the turnover frequency TOF shown in Equation 1.

$$TOF = \frac{\dot{n}_{product}}{n_{catalyst}} \quad (1)$$

Since the molar flow of product cannot be determined in high accuracy due to a change of the total flow caused by the condensation of water before the dry gas was flowing through the online IR-analyzer, the TOF has to be modified according to Equation 2.

$$TOF = \frac{\dot{n}_{substrate} \cdot X_{substrate}}{n_{catalyst}} \quad (2)$$

The substrate (CO) molar flow can easily be calculated from the volume flow of the calibrated MFC. Since the condensation of water takes place in both operating modes (bypass measurement and reactor measurement), it does not affect the measured values anymore, so that the conversion can directly be calculated. The molar value of the catalyst is referring to the amount of ruthenium

atoms in the catalyst sample. The maximum overall error for the catalyst activity amounts to ± 5 % and error bars have been omitted in the figures for sake of clarity.

Since the amount of additive is related to the fixed amount of IL which is determined by the pore volume of the support material, the quantity is given as molarity value M. For the sake of clarity, the conversion between molarities and the molar ratio of additive to IL χ is given in Table 1. Additionally, the molar ratio of additive to ruthenium ξ is given as well.

Table 1. Conversion between molarities M of the additive and molar ratio of additive to IL χ. Additionally, the molar ratio of the additive to ruthenium ξ is given.

Molarity M $mol_{additive}\ L_{IL}^{-1}$	Additive to IL ratio χ $mol_{additive}\ mol_{IL}^{-1}$	Additive to Ru ratio ξ $mol_{additive}\ mol_{Ru}^{-1}$
0	0.00	0.00
0.25	0.04	0.19
1	0.17	0.77
2	0.35	1.54
3	0.52	2.31
4	0.70	3.08
5	0.87	3.86
6	1.04	4.63
7	1.22	5.40
8	1.39	6.17

Spectroscopic evaluation. The DRIFTS measurements were conducted using a dedicated *in situ* infrared (IR) setup described in previous work [31, 34] and shown in Figure S6 of the Supporting Information. Briefly, the setup consists of a high temperature reactor chamber equipped with Praying Mantis diffuse reflectance accessory (both from Harrick). The optical path of the setup is

completely evacuated, which leads to improved long-term stability during the measurements. The temperature of the sample is measured via a type K thermocouple, which is directly in contact with the powder sample. All spectra were measured using a KBr beam splitter and a liquid N_2 HgCdTe detector with a spectral resolution of 2 cm^{-1} and an acquisition time of 1 min. A total of three pressure controllers and five mass flow controllers (Bronkhorst) are employed to adjust the pressure (1 mbar – 20 bars), gas composition and gas flow (0.2 – 20 mL_N min^{-1}). The experimental setup is operated in a completely remote-controlled fashion. This ensures that the pressure and gas composition are set accurately and reproducibly according to the predefined procedure. Ar (Linde, > 99.999 %) was dosed without further purification, CO (Linde, > 99.997 %) was passed through a carbonyl trap (Gaskleen® II Purifier from Pall Corporation) to ensure that the gas feed is free of metal carbonyls. Prior to the experiment, each sample was purged over night with 2 mL_N min^{-1} Ar at 1 bar and 30 °C. The background spectrum was recorded under the same conditions. Subsequently, the catalyst sample was exposed to CO (1 bar, 9 min), evacuated (~1 mbar, 1 min) and exposed to Ar (1 bar, 10 min). This procedure was applied at temperatures between 30 and 120 °C in temperature steps of 30 °C. Maximum standard deviation of this procedure is less than 7 % and error bars have been omitted for sake of clarity. Heating and cooling between the gas exposures was performed with a temperature ramp of 3 °C min^{-1} in Ar (1 bar). Two consecutive heating/cooling cycles were performed for all samples.

Computational details. The DFT calculations were carried out using the TURBOMOLE [35-36] software package. The BP86 [37-38] functional with atom-pairwise ("D3") dispersion corrections [39] was used in combination with the def2-TZVPPD [40-41] basis set, which includes diffuse functions to account for a reasonable description of the anionic species. This kind of an approach has been successfully applied to similar systems. [42-43] Optimizations were carried out without any

constraints and vibrational frequencies were determined using the analytical derivatives of the energy as implemented in the AOFORCE module within TURBOMOLE.

Results and discussion

Due to the fact that the benchmark system already contains ruthenium, we focus on the application of cheap non-noble metal chlorides for the improvement of the CO uptake. As a measure for the catalytic activity, the Ru-based turnover frequency (TOF, see Eq. 1) has been calculated for every system. The basis for the evaluation is a temperature variation experiment at constant feed flows and compositions. Using the example of a 2 M CuCl catalyst, the result of a typical experiment is shown in Figure 1. Turnover frequency (TOF) values are shown as a function of the reaction temperature over the course of the time-on-stream of the continuous catalytic experiment demonstrating good stability of the CuCl-modified system under investigation.

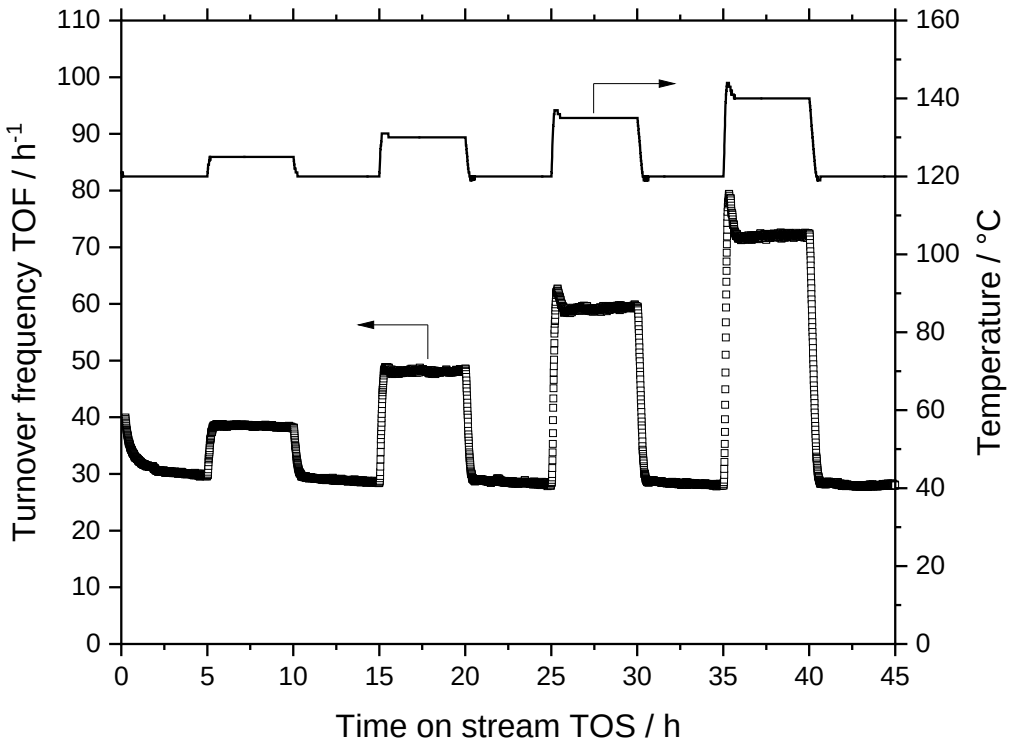

Figure 1. Turnover frequency (TOF) data obtained from a 2 M CuCl-doped SILP WGS catalyst sample. TOF (left y-axis) and temperature in the catalyst bed (right y-axis) are plotted over time-on-stream (TOS) of the continuous experiment. T = 120 – 140 °C, p = 1 bar, precursor = $[Ru(CO)_3(Cl)_2]_2$, loading (Ru) = $0.02 g\, g^{-1}_{Support}$, IL = $[C_4C_1C_1Im]Cl$, α = 0.34, M_{CuCl} = $2\, mol\, L^{-1}_{IL}$, m_{cat} = 2.0 g, p_{H2O}: p_{CO} = 2:1, $\dot{V}_{tot}$ = $174\, mL_N\, min^{-1}$, TOS = 45 h.

From these raw data, an averaged TOF for every temperature stage has been calculated based on the measured steady-state conversion. These data have been transferred into the TOF vs. temperature diagram shown as Figure 2. For each metal chloride doping experiment shown in the Figure, 2.0 g of catalyst sample (molarity of the metal chloride was 2 in all cases; χ = 0.35) was placed in the reactor and tested in a temperature variation experiment (120 °C – 140 °C in 5 °C steps) with a total time on stream (TOS) of 45 h.

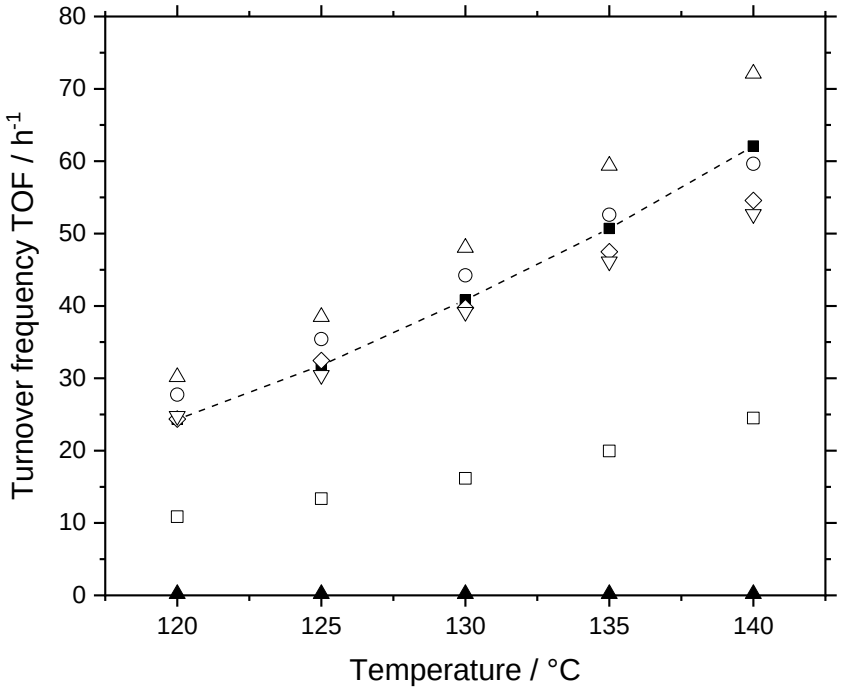

Figure 2. Catalytic results for the WGS experiments with different transition metal chlorides additives ($CuCl$△, $FeCl_2$○, $ZnCl_2$◇, $CoCl_2$▽, $NiCl_2$□) compared to the benchmark SILP experiment (■ with dashed line) and pure CuCl in ionic liquid (▲). Reaction conditions: T = 120 – 140 °C, p = 1 bar, precursor = $[Ru(CO)_3(Cl)_2]_2$, loading (Ru) = $0.02 g\, g^{-1}_{Support}$, IL = $[C_4C_1C_1Im]Cl$,

α = 0.34, $M_{additive}$ = 2 $mol\ L_{IL}^{-1}$, m_{cat} = 2.0 g, p_{H2O}: p_{CO} = 2:1, $\dot{V}_{tot}$ = 174 $mL_N\ min^{-1}$, TOS = 45 h. Maximum error ± 5 %, error bars omitted for sake of clarity.

In this plot, the benchmark system without additives is indicated with a dashed line for better comparability. It can be seen, that the additives used can be subdivided into three groups with respect to their effect on the catalytic performance. Additives of group one show a negative influence, here shown for $NiCl_2$. This compound reduces the activity by - 55 % at 120 °C and by - 61 % at 140 °C compared to the benchmark system. This behavior can be attributed to the fact that $NiCl_2$ added to chloride ILs forms tetrahedral $[NiCl_4]^{2-}$ ions. [44-45] This anionic chlorometallate complex is known to build strong hydrogen bond interactions with the protons at imidazolium cations. By doing so, the imidazolium-ring protons and $[NiCl_4]^{2-}$ions build an extended three-dimensional hydrogen-bond network. [44] We suggest that this leads to a strong decrease of ion mobility, accompanied by a loss in reversible CO binding capacity.

Additives of the second group, containing $ZnCl_2$ and $CoCl_2$ as additives, did not show any effect at low temperatures while they tend to decrease the activity slightly at elevated temperatures (e.g. $ZnCl_2$: - 12 % and $CoCl_2$: - 15 % at 140 °C) in comparison with the benchmark system. The mildly negative influence of these transition metal halides can be explained by the influence of the additive on the IL acidity at higher molar ratio χ of the additive. At these concentrations the additive changes the IL from Lewis-basic (low metal chloride addition; chloride rich IL) to neutral and further to Lewis-acidic (high metal chloride addition; chloride poor IL). [23, 46] This change is coming along with the loss of the IL's ability to reversibly bind CO. [23] For $ZnCl_2$ and $CoCl_2$ this critical neutral regime was determined to be at χ = 0.30 – 0.33. [29-30, 47] Using the example of $ZnCl_2$, in this very narrow neutral zone, an equilibrium of free Cl^-, Lewis-neutral $[ZnCl_4]^{2-}$ and Lewis-acidic $[Zn_2Cl_6]^{2-}$ has been suggested by Taylor et al. [48] Since the value for χ in the screening

experiments is 0.35 (see Table 1), the natures of the Zn and Co-doped ILs are expected to be Lewis-acidic.

Additives of the third group exhibit an overall positive influence, here shown for CuCl and $FeCl_2$. While $FeCl_2$ is showing a catalytic enhancement of +14 % at 120 °C, a slight decrease in activity was measured for 140 °C (- 4 %). CuCl, however, reveals a catalytic improvement of +24 % at 120 °C and +16 % at 140 °C. The positive effect of these two additives can be explained with the physical properties of the generated metal-halide ILs. For both d-block metals, the neutral zone is predicted to be at χ-values > 0.33 so that Lewis-basic or neutral species should be predominant under the applied conditions. [30] In the case of $Fe(II)^+$ containing ILs, however, a temperature depending effect can explain the diminishing positive influence. Sitze et al. suggested the possibility of the formation of higher coordinated Lewis-acidic species such as $[Fe_2Cl_5]^-$ at elevated temperatures. [46] This is in good accordance with the findings of Lecocq et al. who also showed evidence for the formation of higher coordinated species depending on the temperature. [49] Furthermore, Taylor et al. reported an equilibrium between Fe(II) and Fe(III) species. [50] The latter ones are known to form higher coordinated, acidic complex ions which are favored under elevated temperatures. [46] After all, only CuCl seems to have a significant positive effect on the catalyst activity of the Ru-based SILP-catalyzed WGSR over the whole temperature range under investigation. In order to exclude a potential catalytic activity of CuCl itself, a blank SILP catalyst sample was prepared which did not contain any Ru-precursor complex but only the IL and CuCl. As shown in Figure 4, CuCl does not show any WGS activity in our system. Therefore, CuCl seems to act as CO shuttle only and is not forming an active catalyst in absence of the Ru-precursor.

Encouraged by the positive effects found for the CuCl-doped SILP WGS systems, we varied the molar ratio χ in a next set of experiments to check for a correlation between the enhanced catalytic activity and the amount of CuCl present in the catalyst sample. Furthermore, we tried in this way

to maximize the activity boost caused by the CuCl additive. The results from varying the CuCl loading of the catalyst samples are summarized in Figure 3. There is a strong correlation between the CuCl loading of the IL film and the catalytic activity. An increasing activity can be recorded with increasing amount of CuCl until a maximum is reached at the 4 M ($\chi = 0.7$) catalyst sample. At this point, a rise in catalytic performance of +30 % can be realized (at 135 °C) as compared to the benchmark system. From this maximum on, further addition of CuCl leads to a steeply declining activity. In the case of the 6 M sample, a loss of activity by - 43 % (at 120 °C) and - 39 % (at 140 °C) compared to the benchmark system is measured while the 8 M sample is showing even lower values with a decline of - 84 % (at 120 °C) and - 61 % (at 140 °C). Again, the observed behavior can be attributed to a change of the Lewis acid-base behavior of the different chlorocuprate species being formed upon CuCl addition to the IL.

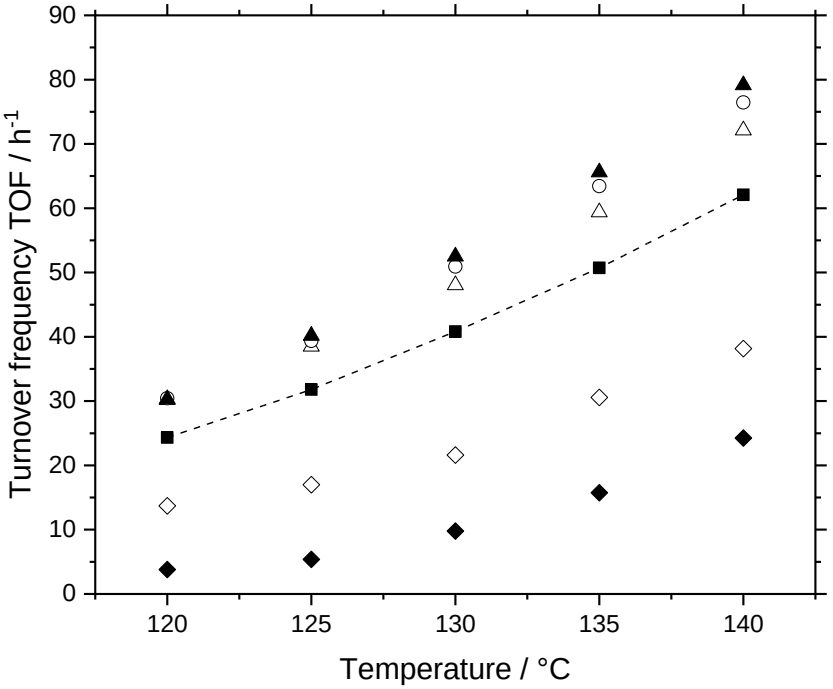

Figure 3. Catalytic results for the variation of the CuCl content in the IL film of the catalyst samples (2 M △, 3 M ○, 4 M ▲, 6 M ◇, 8 M ◆) compared to benchmark (no CuCl ■ with dashed line).

Reaction conditions: T = 120 – 140 °C, p = 1 bar, precursor = $[Ru(CO)_3(Cl)_2]_2$, loading (Ru) = $0.02 g\ g_{Support}^{-1}$, IL = $[C_4C_1C_1Im]Cl$, α = 0.34, M_{CuCl} = $2 - 8\ mol\ L_{IL}^{-1}$, m_{cat} = 2.0 g, p_{H2O}: p_{CO} = 2:1, $\dot{V}_{tot}$ = 1747 $mL_N\ min^{-1}$, TOS = 45 h. Maximum error ± 5 %, error bars omitted for sake of clarity.

Depending on the CuCl content present in the IL film, different complexes form which are in an equilibrium with each other. While complexes with a higher chloride content (lower CuCl loading) form Lewis-basic species, such as $[CuCl_2]^-$ or $[CuCl_3]^{2-}$, which also allow free Cl^- ions to coexist, complex ions with a lower chloride content (higher CuCl loading) form Lewis-acidic species like $[Cu_2Cl_3]^-$ or $[Cu_3Cl_4]^-$ that consume free Cl^- ions by forming neutral chlorocuprate species. [23, 28, 30, 51-52] Such equilibria creating either a chloride-rich (Lewis-basic) or a chloride-poor (Lewis-acidic) environment have been previously reported for other halometallate IL systems. [30, 47, 53] We suggest, that the predominance of Lewis-acidic chlorocuprate species leads to a loss of the IL's ability to reversibly bind CO. Furthermore, it has been shown that free chloride ions play a crucial role in the WGS mechanism. As we showed in a previous study, chloride ions induce the reversible cleavage of the Ru-chloro-carbonyl precursor complex $[Ru(CO)_3(Cl)_2]_2$, which is a mandatory step to form the active species of the reaction. [31] Upon consumption of free chloride by the Lewis-acidic cuprous species, the equilibrium of Ru-chloro-carbonyl species will be shifted to the less active Ru-chloro dimer complex that is less suitable for promoting the WGS reaction.

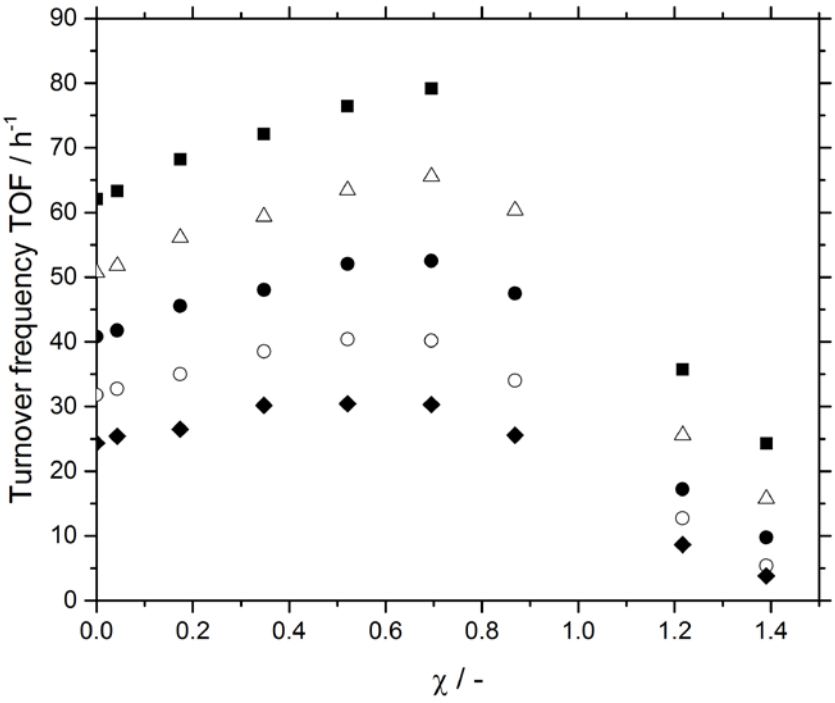

Figure 4. Catalytic results for the variation of the CuCl content in the $[C_4C_1C_1Im]Cl$ film (χ) of the catalyst samples at different temperatures (120 °C ◆, 125 °C ○, 130 °C ●, 135 °C △, 140 °C ■). T = 120 – 140 °C, p = 1 bar, precursor = $[Ru(CO)_3(Cl)_2]_2$, loading (Ru) = $0.02 g\, g_{Support}^{-1}$, IL = $[C_4C_1C_1Im]Cl$, α = 0.34, $M_{CuCl} = 2 - 8\ mol\ L_{IL}^{-1}$, m_{cat} = 2.0 g, p_{H2O}: p_{CO} = 2:1, $\dot{V}_{tot}$ = 1747 $mL_N\, min^{-1}$, TOS = 45 h. Maximum error ± 5 %, error bars omitted for sake of clarity.

To confirm these assumptions, the overall trend for a variation of the CuCl content has to be taken into account at different temperatures. The results of these experiments are given in Figure 4 where the TOF is plotted over the CuCl loading at different temperatures. It can clearly be seen, that the activity of the catalysts is increasing for every temperature with an increasing CuCl loading. At all temperatures, a maximum is being reached at the 4 M doped catalyst (χ = 0.7) confirming the conclusions given above. Interestingly, the transition point from Lewis-basic to Lewis-acidic is reported to be around a molar ratio of CuCl to chloride IL of χ = 1. [23] We found, that this transition range in our application is shifted to around χ = 0.7. We suggest that this deviation can be attributed

to two different effects. First of all, our system does not consist of a pure mixture of CuCl and an imidazolium chloride IL. The active compound we use is a Ru-chloro-carbonyl dimer which needs some chloride ions to form the active species. Therefore the real χ-value in our system is shifted to a higher value. If we assume that every Ru-atom in the mixture is consuming one chloride ion, the theoretical molar ratio of CuCl to IL would shift to $\chi = 0.92$ which is already very close to the transition range given in literature. Furthermore, water is being absorbed by the IL at process conditions of the WGS reaction. As Gazitúa et al. reported, impurities such as water may significantly affect the Lewis acidity or basicity of imidazolium-based ILs. [54] This effect could also play a role concerning the transition range from the basic to the acidic regime in our system.

To verify the improved CO uptake caused by the CuCl additive, we performed CO chemisorption experiments and thermogravimetry analyses (see Figure 5).

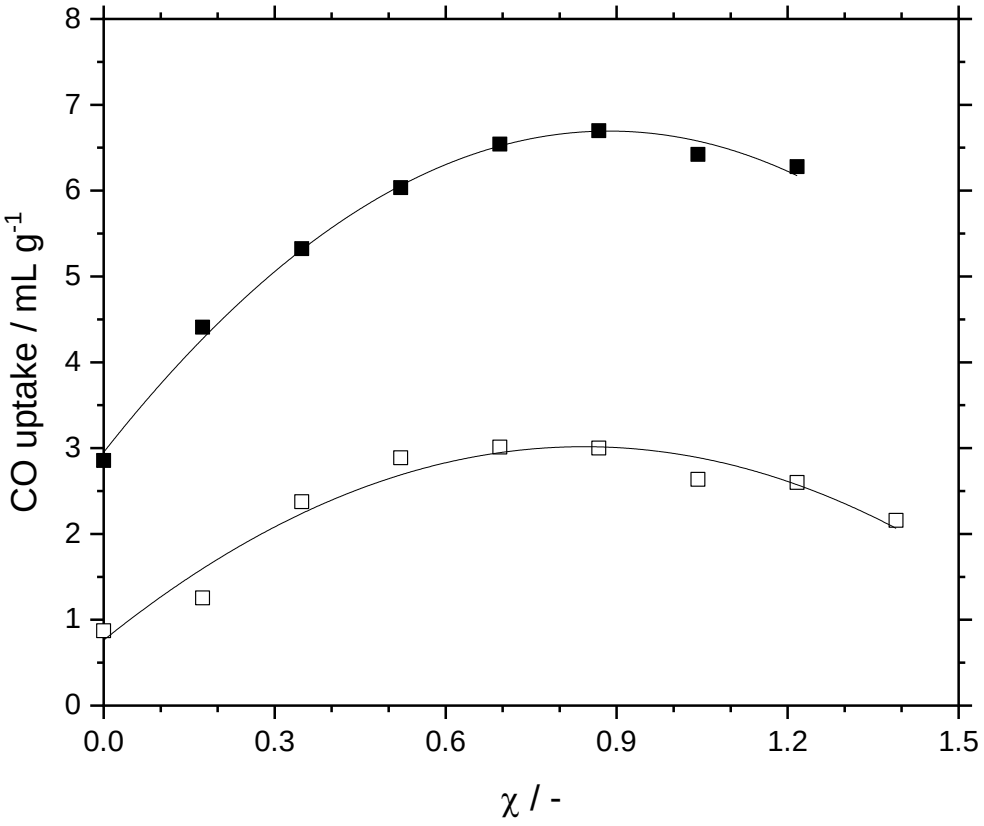

Figure 5. Mass specific volumetric uptake of CO on the dry SILP catalysts (including Ru precursor) at 1 bar and 130 °C as a function of the CuCl content in the $[C_4C_1C_1Im]Cl$ film (χ) obtained by means of pulse chemisorption experiment in an AutoChem analyzer (□) and high-resolution thermogravimetry in a XEMIS sorption analyzer (■). Solid lines are based on second order polynomial fits. Maximum error ± 5 %, error bars omitted for sake of clarity.

Interestingly, both techniques show a maximum of CO uptake in the same region (χ = 0.7 – 0.9). This value is also in good accordance with the maximum catalyst activity throughout the measured temperature ranges (compare to Figure 3). By using the pulse chemisorption setup, the benchmark catalyst system showed a CO sorption of 0.87 $mL_N\ g^{-1}$ while the maximum uptake value is more than tripled to 3.01 $mL_N\ g^{-1}$ (χ = 0.7). With the HR-thermogravimetry setup, a value of 2.85 $mL_N\ g^{-1}$ is obtained for the benchmark catalyst, which is more than doubled to 6.69 $mL_N\ g^{-1}$ at the peak uptake (χ = 0.87). The difference in absolute CO sorption as well as the slight variation of the peak position can be attributed to the different measurement techniques. In the case of the pulse chemisorption experiments, gas sorption cannot reach full equilibrium due to a short contact time of the dosed CO in the helium carrier gas flow. In contrast to this technique, the HR-thermogravimetry setup allows the catalyst systems to reach equilibrium gas uptake (Figure S2), due to the fact that the samples are exposed to a pure CO atmosphere for an extended duration. Further, HRTGA allows for the relation of the CO uptake to the dry mass of catalyst. It has to be pointed out that no adsorption of CO is detected when analyzing SILP catalysts without dissolved Ru-precursor (Figure S3). This finding strongly supports the hypothesis of the different Cu species acting as CO shuttle, transferring CO to the Ru-complex under reaction conditions. Furthermore, it can be denoted, that a CuCl addition also yields a similar trend for the relative amount of adsorbed H_2O in the as-prepared SILP catalysts (see Figure S4).

In a next set of experiments, we investigate selected catalyst samples with DRIFTS to probe whether Cu carbonyls are formed in the Ru-based water gas shift (WGS) catalyst. IR spectroscopy

is highly sensitive towards metal carbonyls. In a recent publication, we employed DRIFTS to differentiate between several $[Ru(CO)_xCl_y]_n$ complexes in the IL phase of a SILP catalyst. [31] We showed that exposure of CO to $[Ru(CO)_3Cl_2]_2/[C_4C_1C_1Im]Cl/Al_2O_3$ leads to the formation of CO-rich Ru complexes with broad vibrational features in the carbonyl region of the IR spectra. In the present study, we conducted DRIFTS experiments with Ru-free samples. This ensures that the carbonyl features originate from Cu carbonyls only. We assign the peak positions obtained experimentally with the help of DFT. In Figure 6a and 6b, we show the spectra of pristine $CuCl/Al_2O_3$ as a reference and $CuCl/[C_4C_1C_1Im]Cl/Al_2O_3$ (4 M doped catalyst showing maximum activity improvement) in 1 bar CO at the temperatures indicated. CO gas phase signals were subtracted using a CO reference spectrum and a low pass filter. Details on the procedure have been described previously. [34, 55] Further post-data treatment includes normalization of the spectra to compensate for changes in the reflectivity induced by heating and baseline correction. [56]

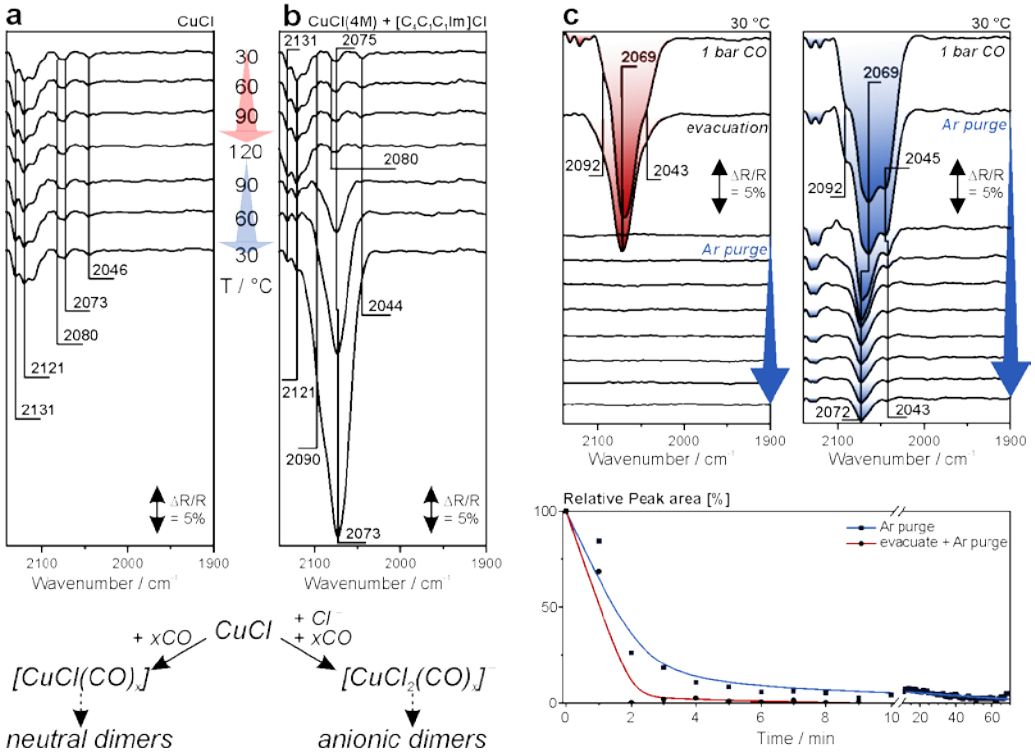

Figure 6. In-situ DRIFTS during exposure of CuCl-modified samples to CO: DRIFT spectra recorded in 1 bar CO on (a) $CuCl/Al_2O_3$ and (b) $CuCl/[C_4C_1C_1Im]Cl/Al_2O_3$ at the temperature indicated; c) DRIFT spectra and evolution of the integrated peak area upon removal of the CO gas phase.

The spectra obtained from the IL-free $CuCl/Al_2O_3$ sample are depicted in Figure 6a. They show features at 2131 and 2121 cm^{-1} and smaller peaks at 2080, 2073 and 2046 cm^{-1}. The intensity of the observed bands does not change during the experiment. The spectra recorded during exposure of $CuCl/[C_4C_1C_1Im]Cl/Al_2O_3$ to CO (Figure 6b) exhibit similar bands. However, the intensity of the features at 2090, 2073 and 2044 cm^{-1} increases drastically upon cooling which is in good accordance with literature stating that the CO complexation is of exothermic nature. [23] We attribute all peaks observed to the formation of Cu carbonyls. Depending on the starting material, it is plausible that Cu monomers, dimers and anionic species are present. [52, 57] In Table 2, we present peak positions derived from DFT calculations for a set of proposed Cu species. Starting from CuCl, the addition of CO leads to formation of neutral monomers $Cu(CO)_xCl$ (**1** – **3** in Table 2). According to DFT, these species exhibit peaks at > 2100 cm^{-1}, which corresponds well with our experimental data. Haakanson et al. precipitated Cu(CO)Cl from organic solutions and reported an intense peak at 2127 cm^{-1}, which is in excellent agreement with the peak center at 2131 cm^{-1} observed during our CO dosing experiments. Therefore, we assign the bands observed for the $CuCl/Al_2O_3$ sample to neutral $Cu(CO)_xCl$ (x = 1 – 3) species.

Table 2. Peak positions of copper carbonyls as derived from DFT. The most intense peak is highlighted in bold.

Index	Species	$\nu(CO)_{DFT}$
	Neutral monomers	
1	$Cu(CO)Cl$	**2109**
2	$Cu(CO)_2Cl$	2120, **2080**
3	$Cu(CO)_3Cl$	2129, **2091**
	Neutral dimers	
4	$[Cu_2(CO)_2(\mu\text{-}Cl)_2]$	**2085**
5	$[Cu_2(CO)_4(\mu\text{-}Cl)_2]$	**2080**, 2107
	Anionic dimers	
6	$[Cu_2(CO)_2(\mu\text{-}Cl)_3]^-$	**2016**
	Anionic monomers	
7	$[Cu(CO)Cl_2]^-$	**2001**
8	$[Cu(CO)_2Cl_2]^-$	**2005**, 2046
	Di-anionic monomers	
9	$[Cu(CO)Cl_3]^{2-}$	**1937**

Additionally, we find an intense peak with contributions at ~2045, ~2070 and ~2090 cm^{-1} for the 4 M doped ($\chi = 0.7$) $CuCl/[C_4C_1C_1Im]Cl/Al_2O_3$ system. Huang et al. identified $[CuCl_2]^-$, $[Cu_2Cl_3]^-$ and $[Cu_3Cl_4]^-$ in a mixture of CuCl and $[C_4C_1Im]Cl$. [52] David et al. studied a mixture of CuCl and $[C_6C_1Im]Cl$ and attributed the observed CO uptake to formation of $[Cu(CO)Cl_3]^{2-}$.[23] Both systems are very close to the Cu-modified WGS catalyst studied in this work. According to our calculations, however, the calculated peak position of $[Cu(CO)Cl_3]^{2-}$ (**9**, 1935 cm^{-1}) matches only poorly the intense band observed in the experiment. A better agreement is found for neutral and anionic Cu dimers as well as for anionic Cu monomers (**4** – **8**, 2085 – 2001 cm^{-1}). As we observe at least three distinct contributions during CO dosing, we propose that several Cu species coexist in the IL phase with neutral species constituting the biggest share. This finding correlates

well with the fact, that the CuCl/IL ratio in the investigated 4 M doped catalyst sample should result in a system being located in the Lewis neutral range (compare Figure 4).

During heating, the spectra of $CuCl/[C_4C_1C_1Im]Cl/Al_2O_3$ undergo only minor changes as compared to the cooling cycle, where the intense bands at < 2100 cm^{-1} evolve. We attribute this induction period to thermally induced changes in the SILP, such as a redistribution of the IL in the pores of the support. During catalyst testing, the WGSR is performed at T > 120 °C. At these elevated temperatures, we observe only comparatively small carbonyl peaks in case of the IL-containing sample. This indicates that the Cu carbonyls are present in low concentration in the SILP at elevated temperatures due to the exothermic nature of their formation. Further, we evaluated the stability of the species by investigating the response of the system to removal of the CO gas phase, i.e., to evacuation and/or Ar purging. In Figure 6c, we compare spectra recorded after exposure to CO (1 bar), evacuation (~1 mbar, 1 min) and purging with Ar with spectra obtained in the same fashion but without the evacuation interval. In the lower panel in Figure 8c we show the development of the corresponding peak areas. Evacuation of the reactor volume leads to immediate loss of all CO bands. In contrast, a weak feature at 2072 cm^{-1} is clearly visible in the spectra obtained after 8 min of Ar purging without evacuation. This underlines our hypothesis that the Cu carbonyls observed are, in general, rather labile species. They decompose in the absence of the CO atmosphere, in particular during evacuation and at elevated temperatures. Note that dynamic formation and decomposition under reaction conditions is essential for the Cu carbonyls to operate as efficient shuttle which provides CO to the Ru catalyst. Due to the fast kinetics of formation and decomposition, comparatively low concentrations of the shuttling species can have a major influence on the catalytic activity of the WGS catalyst.

Conclusion

In this work, we investigated the influence of different non-noble metal chlorides as additives for the SILP-catalyzed, ultra-low temperature WGSR using a Ru-complex as active metal. The purpose of the additives is to enhance the low CO solubility in ILs, for example compared to our benchmark SILP system based on $[C_4C_1C_1Im]Cl$. Testing of different metal halides revealed that CuCl is the additive of choice showing clearly enhanced activity (+30 %) across the entire temperature range under investigation (120 – 140 °C). All other additives showed minor activity improvements or even deactivation compared to the benchmark system (see Figure 4). The CuCl additive leads to a maximum increase in activity (measured as TOF) for the 4 M catalyst sample ($\chi = 0.7$). Further addition of CuCl resulted in a loss of the beneficial effect, whereas the blank test with pure CuCl/IL samples (without Ru) showed no catalytic activity at all. The observed concentration effect on activity can be attributed to the Lewis acid-base properties of the different chlorocuprate species formed and their ability to reversibly bind CO. These chlorocuprate species evolve upon CuCl addition to the imidazolium chloride IL. We explain the activity enhancement and CuCl concentration dependency with the special role of Lewis-basic and neutral chlorocuprate species for shuttling CO to the Ru-complex. This shuttling helps to overcome limitations caused by the limited CO solubility in the IL. In fact, the CuCl-modified systems showed an increased CO uptake with a concentration-dependent maximum located in the same region as the maximum for the catalytic activity (compare Figures 5 and 6).

With the help of DFT calculations and DRIFTS measurements, several chlorocuprate species could be identified. To ensure, that observed carbonyl features originate from Cu carbonyls only, Ru-free samples were investigated. It was shown, that the majority of the present species are neutral $Cu(CO)_xCl$ complexes accompanied by minor amounts of Lewis-basic anionic chlorocuprate

species such as [$Cu(CO)_xCl_2$]. These findings correlate well with the proposed shuttling effect of chlorocuprate species in the active WGS SILP system.

In general, this study shows that the SILP technology holds potential for further optimization by additive addition to the supported IL film. Such improvements are of high importance for large-scale SILP applications, since they allow reducing the amount of catalyst material or the content of expensive transition metal species while maintaining the same performance of the WGS reactor and CO clean-up unit.

Acknowledgements

The authors gratefully acknowledge funding by the European Commission within the Horizon 2020-SPIRE project ROMEO (grant agreement number 680395). Additional support by the DFG is acknowledged from the Excellence Cluster “Engineering of Advanced Materials” (Bridge Funding) and by the Free State of Bavaria through its funding for the *Energie Campus Nürnberg* (www.encn.de).

References

[1]. Baerns, M.; Behr, A.; Brehm, A.; Gmehling, J.; Hinrichsen, K.-O.; Hofmann, H.; Onken, U.; Palkovits, R.; Renken, A., *Technische Chemie*. 2nd ed.; Wiley-VCH: **2013**; p 736.
[2]. Schödel, N., Industrial Hydrogen and Syngas Production - State of the Art and New Development, *Erdöl Erdgas Kohle* **2016,** 132 (2), 70-75.
[3]. Jess, A.; Wasserscheid, P., *Chemical Technology - An Integrated Textbook*. Wiley VCH: **2013**.
[4]. Stolten, D.; Emonts, B., *Hydrogen Science and Engineering : Materials, Processes, Systems and Technology*. **2016**.
[5]. Jacobs, G.; Davis, B.H. In *Catalysis*, **2007**; pp 122-285.
[6]. Behr, A.; Agar, D.W.; Jörissen, J., *Einführung in die Technische Chemie*. Springer Spektrum: **2016**; p 316.
[7]. Werner, S.; Szesni, N.; Kaiser, M.; Fischer, R.W.; Haumann, M.; Wasserscheid, P., Ultra-Low-Temperature Water-Gas Shift Catalysis using Supported Ionic Liquid Phase (SILP) Materials, *ChemCatChem* **2010,** 2 (11), 1399-1402.

[8]. Riisager, A.; Fehrmann, R.; Haumann, M.; Wasserscheid, P., Supported Ionic Liquid Phase (SILP) Catalysis: An Innovative Concept for Homogeneous Catalysis in Continuous Fixed-Bed Reactors, *European Journal of Inorganic Chemistry* **2006,** 2006 (4), 695-706.
[9]. Mehnert, C.P., Supported ionic liquid catalysis, *Chemistry* **2004,** 11 (1), 50-6.
[10]. Steinruck, H.P.; Libuda, J.; Wasserscheid, P.; Cremer, T.; Kolbeck, C.; Laurin, M.; Maier, F.; Sobota, M.; Schulz, P.S.; Stark, M., Surface science and model catalysis with ionic liquid-modified materials, *Adv Mater* **2011,** 23 (22-23), 2571-87.
[11]. Lei, Z.; Dai, C.; Chen, B., Gas solubility in ionic liquids, *Chem Rev* **2014,** 114 (2), 1289-326.
[12]. Ohlin, C.A.; Dyson, P.J.; Laurenczy, G., Carbon monoxide solubility in ionic liquids: determination, prediction and relevance to hydroformylation, *Chem Commun (Camb)* **2004,** (9), 1070-1.
[13]. Kohl, A.L.; Riesenfeld, F.C., *Gas purification*. New York, McGraw-Hill: **1960**; p 556.
[14]. Hogendoorn, J.A.; Van Swaaij, W.P.M.; Versteeg, G.F., The absorption of carbon monoxide in COSORB solutions: absorption rate and capacity, *The Chemical Engineering Journal and the Biochemical Engineering Journal* **1995,** 59 (3), 243-252.
[15]. D. J. Haase, D.G.W., COSORB Process, *Chemical Engineering Progress* **1974,** 70 (5), 74-77.
[16]. Dutta, N.N.; Patil, G.S., Developments in CO separation, *Gas Separation & Purification* **1995,** 9 (4), 277-283.
[17]. Gholap, R.V.; Chaudhari, R.V., Absorption of carbon monoxide with reversible reaction in cualcl4-toluene-complex solutions, *The Canadian Journal of Chemical Engineering* **2009,** 70 (3), 505-510.
[18]. Kasuya, F.; Tsuji, T., High purity CO gas separation by pressure swing adsorption, *Gas Separation & Purification* **1991,** 5, 242-246.
[19]. Yang, R.T., *Adsorbents: Fundamentals and Applications*. John Wiley & Sons: New Jersey, **2003**.
[20]. Benner, L.S.; Balch, A.L., Novel reactions of metal-metal bonds. Insertion of isocyanides and carbon monoxide into the palladium-palladium bond of some palladium(I) dimers, *Journal of the American Chemical Society* **1978,** 100 (19), 6099-6106.
[21]. Komatsu, T.; Hasegawa, E.; Kumamoto, S.-I.; Nishide, H.; Tsuchida, E., Kinetics of binding of O2and CO to 'double-sided' porphyrinatoiron(II) complexes, *J. Chem. Soc., Dalton Trans.* **1991,** (12), 3281-3284.
[22]. Tyeklar, Z.; Jacobson, R.R.; Wei, N.; Murthy, N.N.; Zubieta, J.; Karlin, K.D., Reversible reaction of dioxygen (and carbon monoxide) with a copper(I) complex. X-ray structures of relevant mononuclear Cu(I) precursor adducts and the trans-(.mu.-1,2-peroxo)dicopper(II) product, *Journal of the American Chemical Society* **1993,** 115 (7), 2677-2689.
[23]. David, O.C.; Zarca, G.; Gorri, D.; Urtiaga, A.; Ortiz, I., On the improved absorption of carbon monoxide in the ionic liquid 1-hexyl-3-methylimidazolium chlorocuprate, *Separation and Purification Technology* **2012,** 97, 65-72.
[24]. Mori, M., On Some Dark-colored Chlorocuprates(I, II) and Related Compounds. I. The Method of Preparation and Some Properties, *Bulletin of the Chemical Society of Japan* **1960,** 33 (7), 985-988.
[25]. Axtell, D.D.; Good, B.W.; Porterfield, W.W.; Yoke, J.T., Fused salts at room temperature. Vibrational spectroscopic and other studies of liquid chlorocuprates(I), *Journal of the American Chemical Society* **1973,** 95 (14), 4555-4559.

[26]. Lipshutz, B.H.; Parker, D.; Kozlowski, J.A.; Miller, R.D., Coupling reactions of higher order cuprates with primary halides: extremely mild and efficient substitution reactions of bromides and chlorides, *The Journal of Organic Chemistry* **1983,** 48 (19), 3334-3336.
[27]. Massacesi, M.; Ponticelli, G.; Puggioni, G.; Devoto, G., Halocuprate(II) complexes with isoxazolium and imidazolium derivatives, *Transition Metal Chemistry* **1985,** 10 (4), 149-151.
[28]. Bolkan, S.A.; Yoke, J.T., Room Temperature Fused Salts Based on Copper(I) Chloride - 1-Methyl-3-ethylimidazoium Chloride Mixtures. 1. Physical Properties, *Journal of Chemical & Engineering Data* **1986,** 31 (2), 194-197.
[29]. Scheffler, T.B.; Thomson, M.S., Novel Ambient Temperature Ionic Liquids Formulated from 1-Methyl-3-ethylimidazolium Chloride and Anhydrous Metal Chloride Salts other than Aluminum Chloride, *ECS Proceedings Volumes* **1990,** 1990-17, 281-289.
[30]. Brown, L.C.; Hogg, J.M.; Swadzba-Kwasny, M., Lewis Acidic Ionic Liquids, *Top Curr Chem (Cham)* **2017,** 375 (5), 78.
[31]. Bauer, T.; Stepic, R.; Wolf, P.; Kollhoff, F.; Karawacka, W.; Wick, C.R.; Haumann, M.; Wasserscheid, P.; Smith, D.M.; Smith, A.-S.; Libuda, J., Dynamic equilibria in supported ionic liquid phase (SILP) catalysis: in situ IR spectroscopy identifies [Ru(CO)xCly]n species in water gas shift catalysis, *Catalysis Science & Technology* **2018,** 8 (1), 344-357.
[32]. Bauwesen, N., Determination of the degree of dispersion of metals using chemisorption - Part 3: Flow method. V., D.I.f.N.e., Ed. Beuth Verlag: 2007; Vol. DIN 66136.
[33]. Minnick, D.L.; Turnaoglu, T.; Rocha, M.A.; Shiflett, M.B., Review Article: Gas and vapor sorption measurements using electronic beam balances, *Journal of Vacuum Science & Technology A: Vacuum, Surfaces, and Films* **2018,** 36, 050801.
[34]. Bauer, T.; Maisel, S.; Blaumeiser, D.; Vecchietti, J.; Taccardi, N.; Wasserscheid, P.; Bonivardi, A.; Görling, A.; Libuda, J., Operando DRIFTS and DFT Study of Propane Dehydrogenation over Solid- and Liquid-Supported GaxPty Catalysts, *ACS Catalysis* **2019,** 9 (4), 2842-2853.
[35]. *TURBOMOLE V6.6* http://www.turbomole.com, 2014.
[36]. Ahlrichs, R.; Bär, M.; Häser, M.; Horn, H.; Kölmel, C., Electronic structure calculations on workstation computers: The program system turbomole, *Chemical Physics Letters* **1989,** 162 (3), 165-169.
[37]. Becke, A.D., Density-functional exchange-energy approximation with correct asymptotic behavior, *Physical Review A* **1988,** 38 (6), 3098-3100.
[38]. Perdew, J.P., Density-functional approximation for the correlation energy of the inhomogeneous electron gas, *Physical Review B* **1986,** 33 (12), 8822-8824.
[39]. Grimme, S.; Antony, J.; Ehrlich, S.; Krieg, H., A consistent and accurate ab initio parametrization of density functional dispersion correction (DFT-D) for the 94 elements H-Pu, *J Chem Phys* **2010,** 132 (15), 154104.
[40]. Weigend, F.; Ahlrichs, R., Balanced basis sets of split valence, triple zeta valence and quadruple zeta valence quality for H to Rn: Design and assessment of accuracy, *Phys Chem Chem Phys* **2005,** 7 (18), 3297-305.
[41]. Hellweg, A.; Rappoport, D., Development of new auxiliary basis functions of the Karlsruhe segmented contracted basis sets including diffuse basis functions (def2-SVPD, def2-TZVPPD, and def2-QVPPD) for RI-MP2 and RI-CC calculations, *Phys Chem Chem Phys* **2015,** 17 (2), 1010-7.
[42]. Stepic, R.; Wick, C.R.; Strobel, V.; Berger, D.; Vucemilovic-Alagic, N.; Haumann, M.; Wasserscheid, P.; Smith, A.S.; Smith, D.M., Mechanism of the Water-Gas Shift Reaction Catalyzed by Efficient Ruthenium-Based Catalysts: A Computational and Experimental Study, *Angew Chem Int Ed Engl* **2019,** 58 (3), 741-745.

[43]. Sobota, M.; Schernich, S.; Schulz, H.; Hieringer, W.; Paape, N.; Wasserscheid, P.; Gorling, A.; Laurin, M.; Libuda, J., Preparation and characterization of ultrathin [Ru(CO)3Cl2]2 and [BMIM][Tf2N] films on Al2O3/NiAl(110) under UHV conditions, *Phys Chem Chem Phys* **2012,** 14 (30), 10603-12.
[44]. Hitchcock, P.B.; Seddon, K.R.; Welton, T., Hydrogen-bond acceptor abilities of tetrachlorometalate(II) complexes in ionic liquids, *Journal of the Chemical Society, Dalton Transactions* **1993,** (17).
[45]. Zhong, C.; Sasaki, T.; Tada, M.; Iwasawa, Y., Ni ion-containing ionic liquid salt and Ni ion-containing immobilized ionic liquid on silica: Application to Suzuki cross-coupling reactions between chloroarenes and arylboronic acids, *Journal of Catalysis* **2006,** 242 (2), 357-364.
[46]. Sitze, M.S.; Schreiter, E.R.; Patterson, E.V.; Freeman, R.G., Ionic Liquids Based on FeCl3and FeCl2. Raman Scattering and ab Initio Calculations, *Inorganic Chemistry* **2001,** 40 (10), 2298-2304.
[47]. Estager, J.; Nockemann, P.; Seddon, K.R.; Swadzba-Kwasny, M.; Tyrrell, S., Validation of speciation techniques: a study of chlorozincate(II) ionic liquids, *Inorg Chem* **2011,** 50 (11), 5258-71.
[48]. Taylor, A.W.; Men, S.; Clarke, C.J.; Licence, P., Acidity and basicity of halometallate-based ionic liquids from X-ray photoelectron spectroscopy, *RSC Advances* **2013,** 3 (24).
[49]. Lecocq, V.; Graille, A.; Santini, C.C.; Baudouin, A.; Chauvin, Y.; Basset, J.M.; Arzel, L.; Bouchu, D.; Fenet, B., Synthesis and characterization of ionic liquids based upon 1-butyl-2,3-dimethylimidazolium chloride/ZnCl2, *New Journal of Chemistry* **2005,** 29 (5).
[50]. Taylor, A.W.; Qiu, F.; Villar-Garcia, I.J.; Licence, P., Spectroelectrochemistry at ultrahigh vacuum: in situ monitoring of electrochemically generated species by X-ray photoelectron spectroscopy, *Chem Commun (Camb)* **2009,** (39), 5817-9.
[51]. Lü, R.; Tangbo, H.; Cao, Z., Ab Initio Calculation of Room Temperature Ionic Liquid 1-Ethyl-3-Methyl-Imidazolium Chlorocuprate (I), *Journal of Natural Gas Chemistry* **2007,** 16 (1), 70-77.
[52]. Huang, C.; Chen, B.; Zhang, J.; Liu, Z.; Li, Y., Desulfurization of Gasoline by Extraction with New Ionic Liquids, *Energy & Fuels* **2004,** 18 (6), 1862-1864.
[53]. Hussey, C.L., Room-Temperature Haloaluminate Ionic Liquids - Novel Solvents for Transition-Metal Solution Chemistry, *Pure Appl Chem* **1988,** 60 (12), 1763-1772.
[54]. Gazitua, M.; Fuentealba, P.; Contreras, R.; Ormazabal-Toledo, R., Lewis Acidity/Basicity Changes in Imidazolium Based Ionic Liquids Brought About by Impurities, *J Phys Chem B* **2015,** 119 (41), 13160-6.
[55]. Kaftan, A.; Schönweiz, A.; Nikiforidis, I.; Hieringer, W.; Dyballa, K.M.; Franke, R.; Görling, A.; Libuda, J.; Wasserscheid, P.; Laurin, M.; Haumann, M., Supported homogeneous catalyst makes its own liquid phase, *Journal of Catalysis* **2015,** 321, 32-38.
[56]. Xu, T.; Schwarz, M.; Werner, K.; Mohr, S.; Amende, M.; Libuda, J., The surface structure matters: thermal stability of phthalic acid anchored to atomically-defined cobalt oxide films, *Phys Chem Chem Phys* **2016,** 18 (15), 10419-27.
[57]. Pike, R.D., Structure and Bonding in Copper(I) Carbonyl and Cyanide Complexes, *Organometallics* **2012,** 31 (22), 7647-7660.